

Quantitative T1 and T2 measurements of tissue characteristics in myocardial infarction – pilot results at 3T

S. K. Piechnik¹, E. Dall'Armellina¹, V. M. Ferreira¹, L. E. Cochlin², J. E. Schneider¹, S. Neubauer¹, and M. D. Robson¹

¹Cardiovascular Medicine, OCMR, Oxford University, Oxford, Oxfordshire, United Kingdom, ²Dept of Physiology, Anatomy and Genetics, Oxford University, Oxford, Oxfordshire, United Kingdom

INTRODUCTION: Late Gadolinium Enhancement (LGE) CMR is the gold standard of imaging irreversible damage in myocardial infarction. However, limitations include invasive contrast administration and sensitivity to accurate choice of Inversion Time (TI). Alternative non-invasive quantitative mapping of the myocardium has been demonstrated to distinguish pathophysiological changes in acute myocardial infarction at 1.5T [1]. We present preliminary experiences of experimental T₁ [2, 3] and T₂ [4] mapping techniques at 3T to distinguish areas of affected from unaffected myocardium.

METHODS: Clinical Material and Methods: 4 patients with a first acute myocardial infarction (age 53±10 years; 3 males) underwent CMR imaging at 3T (TRIO, SIEMENS). LGE images were obtained 24-48 hours post acute infarct [5]; T₁ and T₂ maps were obtained 5-17 days after the ischemic event. Pilot T₁-maps using the novel ShMOLLI sequence (a shortened version of MOLLI [1]) and T₂-maps [4] at a single representative slice were generated. ShMOLLI was implemented as 3 IR experiments split over 9 heartbeats (separated by only one heartbeat) to collect 5+1+1 SSFP images with varying TI (typically 110-5000ms, TE=1.1ms, flip angle=35°, FOV=360x280mm, matrix 192x144, interpolation=2, pixel size~0.9mm). ShMOLLI samples from the second and third IR are taken into account only if the estimated T₁ is shorter than the R-R interval, and they improve nonlinear fit. The nonlinear fitting was implemented in C++ directly in the scanner reconstruction pipeline utilizing parallel processing with images available for viewing directly on console immediately after acquisition. T₂ maps were generated from a series of 5 T₂ prepared images (TE=0, 32, 55, 78, 100ms), also reconstructed directly on the scanner. Imaging parameters: T₂-prepared with single shot SSFP acquisition, TR/TE=313/1.04ms, flip angle 48°, FOV 370x270, acquisition matrix 128x116 interpolation=2, pixel size~1.1mm. Post-processing involved manual segmentation of the myocardium followed by calculation of the distribution of T₁ and T₂ relaxation times. These were fitted into 2 component Gaussians (See Fig. 1) to separately estimate the distributions for affected and unaffected myocardium.

Phantom verification: Both ShMOLLI and T₂ prep-SSFP were validated using separate sets of 50ml Agarose+NiCl gel phantoms [6] with T₂~60ms and T₁ 70-2300ms (for ShMOLLI) and T₁=900-1500ms, T₂=30-100ms (for T₂Prep-SSFP). For T₁ reference we used a spin echo sequence with TI=33, 100, 300, 900, 2700, 5000 ms, TE/TR=6.3ms/10s. For T₂ estimation we used Spin Echo with TR=100ms and TE=6.3, 12, 24, 40, 80, 150, 250, 500ms. Reference images were fitted offline using non-linear methods separately for T₁ and T₂. The average estimates of the phantoms were used as baseline to obtain empirical correction for the *in-vivo* measurements.

RESULTS&DISCUSSION: Phantom study showed that T₁-mapping using ShMOLLI underestimates T₁ values by ~4%. T₂-mapping using T₂-prep has relatively poor metrological properties as identified by the empirical relationship: $T_{2prep}=0.8*T_{2reference}+20ms$; ($R^2=0.9$). These corrections have been used to present the measured relaxation times in Table 1. The application of the methods in clinical cases was easy due to short imaging times. T₁ maps were of good quality and showed distinctly separate distribution peaks within the myocardium (Fig. 1A). T₂ maps were less robust but, with the exception of case #3 which was affected by a large artefact in the anterolateral wall, it was possible to assess the entire myocardial rim and obtain similar bimodal histograms. LGE lesions overlapped with areas characterized by increased relaxation times in the quantitative maps (Fig.1, inserts). Average T₁ estimates in the peaks for “affected” and “unaffected” myocardium were consistent between cases (CV=3% and 2% respectively). Inter subject variability of T₂ was larger (CV=4 and 7% respectively). The width of estimated peaks was about 4-5% of the average estimates. This compares favourably to the estimated relative changes in the relaxation times (15-25% for T₁; 26-60% for T₂), making relaxation maps a good target for automated objective lesion segmentation.

Conclusion: T₁ and T₂ relaxation times in infarcted myocardium demonstrate distinctively separate distribution peaks that co-localise with LG enhanced regions of damage. While the underlying pathophysiological phenomena mirrored in relaxation properties remain to be established, this observation potentially paves the way to objective lesion segmentation without the need for contrast agents.

Acknowledgments: This research was funded by NIHR Biomedical Research Centre Programme

References: [1] Blume. J Magn Reson Imaging 2009. 29:480-7. [2] Piechnik. 26th Annual Scientific Meeting, ESMRMB 2009. 485. [3] Messroghli. Magn Reson Med 2004. 52:141-6. [4] Giri. Journal of Cardiovascular Magnetic Resonance 2009. 11:O4. [5] Kim. N Engl J Med 2000. 343:1445-53. [6] Cochlin. Proceedings of 11th Annual ISMRM Meeting 2003. 885.

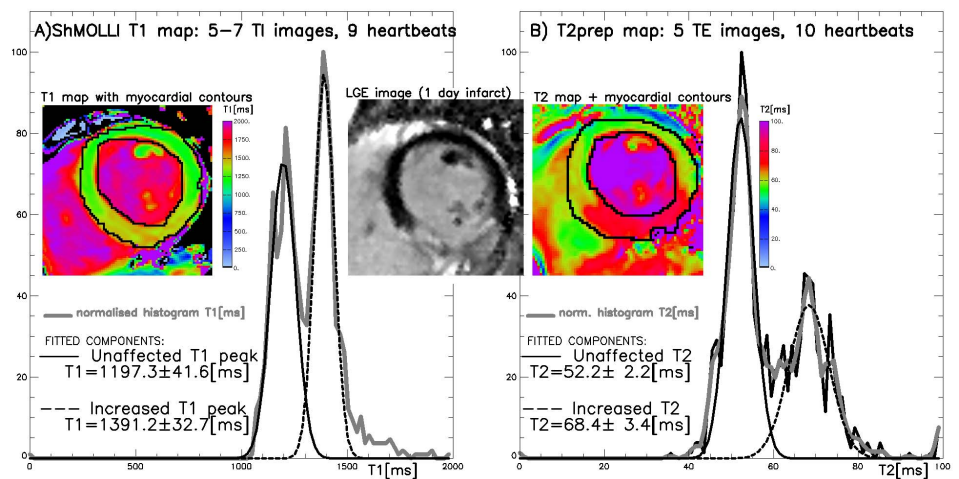


Fig. 1. The distributions of the measured (non-corrected) quantitative relaxation times obtained in patient #1 show clear peaks distinguishing unaffected from affected myocardium using both A) T₁ and B) T₂ maps. (Relaxation maps shown in coloured inserts; LGE in grey scale.)

Table 1. Corrected estimates of the relaxation times in all studied cases.

Case	T1[ms]			T2[ms]			Infarct age days
	unaffected	affected	Change	unaffected	affected	Change	
#1: F(50)	1243.3±47	1452.7±45	16.84%	40.3±3	60.5±4	50.24%	5
#2: M(49)	1308.6±63	1493.3±55	14.12%	42.1±4	58.4±3	38.73%	15
#3: M(68)	1284.1±51	1500.1±60	16.82%	37.9±2	47.8±2	26.21%	17
#4: M(45)	1217.0±57	1522.8±71	25.13%	36.2±4	57.8±4	59.47%	15
Overall	1263±41	1492±29	18±5%	39±3	56±6	44±14%	12±5